Simulation of active tectonic processes for a convecting mantle with moving continents

Valeriy Trubitsyn,[1,2] Mikhail Kaban,[1] Walter Mooney,[3] Christoph Reigber[1] and Peter Schwintzer[1,]*

[1] *GeoForschungsZentrum, Potsdam, Germany. E-mail: kaban@gfz-potsdam.de*
[2] *Institute of Physics of the Earth, Moscow, Russia*
[3] *US Geological Survey, Menlo Park, USA*

SUMMARY

Numerical models are presented that simulate several active tectonic processes. These models include a continent that is thermally and mechanically coupled with viscous mantle flow. The assumption of rigid continents allows use of solid body equations to describe the continents' motion and to calculate their velocities. The starting point is a quasi-steady state model of mantle convection with temperature/pressure-dependent viscosity. After placing a continent on top of the mantle, the convection pattern changes. The mantle flow subsequently passes through several stages, eventually resembling the mantle structure under present-day continents: (a) Extension tectonics and marginal basins form on boundary of a continent approaching to subduction zone, roll back of subduction takes place in front of moving continent; (b) The continent reaches the subduction zone, the extension regime at the continental edge is replaced by strong compression. The roll back of the subduction zone still continues after closure of the marginal basin and the continent moves towards the upwelling. As a result the ocean becomes non-symmetric and (c) The continent overrides the upwelling and subduction in its classical form stops. The third stage appears only in the upper mantle model with localized upwellings.

Key words: continental evolution, mantle convection, marginal basin, subduction.

GJI Tectonics and geodynamics

INTRODUCTION

Over the past few decades, great progress has been made in understanding active tectonic processes based on field observations. However, up to now the theories are more or less phenomenologically based, and are unable to explain the underlying mechanism of many tectonics processes. Only some initial ideas for explaining the temporal evolution and variability of the plate tectonic patterns have been given. Duncan & Turcotte (1994) considered the evolution with time as a stochastic process, which is related to collisions of the continents and randomly appearing mantle plumes. According to Stein & Hofmann (1994) and Condie (1998) mantle convection patterns are quasi-periodical, with the main episodes associated with mantle overturns that are responsible for principal orogenic events. However, these theories give no quantitative insight into the reorganization of the underlying mantle convection. Besides random fluctuations, global mantle evolution shows some regularities, which follow from fundamental equations of energy, mass and momentum conservation. Thus, one of the main tasks of numerical modelling is to find the source for significant transitions in mantle convection.

In this study a simplified numerical model is developed that simulates the main stages of the continental evolution and mechanism of mantle convection's reorganization under the influence of floating continents, that is, thick continental lithosphere with lateral motion.

One of the principal results in the last 15 yr is the concept that continents do not only follow mantle flow, but in return have an impact on the flow. In this way, the continents play an important role in the tectonic history of the Earth (e.g. Gurnis 1988; Lowman & Jarvis 1995, 1999; Trubitsyn & Rykov 1995, 2000). The oldest parts of the continents, with deep lithospheric roots, preserve its structure over billions of years and during that time they are mechanically coupled with the viscous mantle flow and inevitably modify the convection pattern. It is also important that the continental lithosphere, through the thermal blanket effect, causes a warming of the sublithospheric mantle with subsequent upwelling (Arnold *et al.* 2001). This upwelling force tends to increase with time and finally breaks up the large continental plate into several parts. This idea is confirmed by numerical simulations: the existing planar and spherical models are able to describe self-consistently an aggregation of several continents into one supercontinent followed by its break-up and the formation of oceans, and some other events related to the Wilson cycle (Zhong & Gurnis 1993; Lowman & Jarvis 1995; Trubitsyn 2000b; Trubitsyn *et al.* 2003).

*Posthumous contribution.

Therefore, to model the evolution of mantle convection and global tectonic changes one has to consider the role of floating continents. Even a motionless continent affects mantle convection due to thermal and mechanical coupling with the mantle (Nakakuki *et al.* 1997), in particular, through the discontinuities at continental boundaries that may induce small-scale convection flow (King & Ritsema 2000).

The impact of moving oceanic and continental plates on mantle convection was modelled initially by introducing effective boundary conditions that pre-define near-surface mantle velocities (Olson & Corcos 1980; Davies 1988). Such an approach explains some phenomena of plate tectonics, but does not allow the prediction of plate velocities self-consistently as a model result.

Gurnis (1988) created the first model that provides a quantitative description of the continent aggregation and subsequent break-up. Gurnis' approach was further developed by Gurnis & Zhong (1991), King *et al.* (1992), Zhong & Gurnis (1993, 1995). The formation and stability of continental crustal-like piles was modelled in a series of papers by Lenardic, Kaula and Moresi (e.g. Lenardic & Kaula 1995; Lenardic & Moresi 1999).

Numerical modelling of the lithosphere–mantle system by treating this as a fluid-dynamical system is performed by Schott *et al.* (2000). The authors showed that crustal and mantle rheologies and thermal and compositional buoyant forces play the dominant roles in explaining the dynamics in a self-consistent manner.

Gable *et al.* (1991) determined plate velocities by applying force balance conditions at the plate bottom. This method has been extended by Trubitsyn & Rykov (1995) and Trubitsyn (2000b), these authors used Newton's and Euler's solid body equations for 2-D and 3-D spherical models to describe motion of a thick continental plate. This approach is used in the present paper.

In most of the above-mentioned studies no difference between oceanic and continental plates is made, assuming that both interact only at active continental boundaries and are rigidly tied together at passive boundaries. However, there are principal differences between oceanic lithosphere and the old parts of the continents that have deep lithospheric roots. The oceanic plates are generated by mantle material originating from the mid-oceanic ridges and participate in global mantle circulation with a lifetime of less than 200 Myr. Old continental cratons were formed as a result of compositional stratification during the early stages of the Earth's evolution. Despite the fact that these are much colder than the surrounding mantle, the cratons are in equilibrium with the surrounding mantle and remain stable for billions of years. This is explained by Jordan (1978) who postulated the isopycnic (equal-density) hypothesis according to which the density increase caused by low temperatures is compensated by a density decrease due to a compositional difference (i.e. chemical depletion, mainly in Fe and Al) of the roots with respect to the surrounding mantle. This hypothesis is now proved by experimental studies of cratonic peridotites (e.g. Griffin *et al.* 1999) and by the gravity modelling of the continental lithosphere (Kaban *et al.* 2003). Thus, for a numerical simulation extending over several hundred millions of years, one should take into account the principal difference between continental and oceanic plates.

Our modelling approach implies rigid bodies simulating continental plates floating within high viscous oceanic lithosphere. We consider the continents as rigid plates that remain undeformed during the Earth's evolution. This simplified approach enables the investigation of the general aspects of mantle–continent interaction.

The assumption of rigid continents allows the use of Newton and Euler's solid body equations to describe the continents' motion and to calculate their velocities for the 2-D and spherical models correspondingly. The approach follows the one given in Trubitsyn

(2000b). There, the governing equations for mantle convection are supplemented by the equations for moving continents thermally and mechanically coupled with mantle flow. The model was applied to describe in a generalized manner the process of the supercontinent's formation and its subsequent break-up for two thick continents in 2-D model and for eight spherical caps floating on spherical mantle (Trubitsyn 2000b; Trubitsyn *et al.* 2003). In the present paper we investigate the principal stages that are likely to appear in the long-term evolution of moving continents and its effect on the underlying mantle flow. There exist several types of active continental boundaries, typically associated with eastern Eurasia (subduction and backarc basin), South America (subduction and strong compression, absence of a backarc basin) and Western North America (mid-oceanic ridge approaches subduction and submerges under the continent). Our goal is to determine whether these types could represent a logical sequence in the continental evolution or appear in an uncontrolled and arbitrary manner.

WHOLE-MANTLE AND UPPER-MANTLE CONVECTION MODELS

Two general models are usually used to study mantle dynamics: the whole mantle and the upper mantle convection models (Schubert *et al.* 2001). Though many convection models include phase transitions allowing partial layering, present-day simulation technique is not so advanced to combine these models into a comprehensive one. For example, subduction zones and mid-oceanic ridges are important features of the Earth's tectonics. The whole-mantle model implies strong downwellings, but implementation of the internal heating leads to unrealistically wide upwellings. Relatively narrow mid-oceanic ridges are probably passive in most cases and controlled by near surface processes. Future general models, which could describe self-consistently all observables, is just in the initial development stage (Tackley 2000a,b; Zhong *et al.* 2000). As the first approximation, the total mantle convection may be considered as a superposition of mostly whole mantle convection with some critical features in the upper mantle. In the present paper we consider two models with the parameters, which correspond to the whole mantle and to the upper mantle convection separately.

An intensity of the thermal convection is usually characterized by Rayleigh number (Ra). There are three different forms of Rayleigh number depending on the heating conditions: yy

$$Ra_{\mathrm{T}} = (\alpha \rho g \Delta T D^3)/(\kappa \eta), \ Ra_{\mathrm{q}} = (\alpha \rho g q D^4)/(k\kappa \eta),$$
$$Ra_{\mathrm{H}} = (\alpha g \rho^2 H D^5)/(k\kappa \nu), \tag{1}$$

These definitions correspond to the cases when the temperature difference ΔT, surface heat flux q or internal heat production H are considered as the main parameter (Schubert *et al.* 2001). α is thermal expansion coefficient; ρ is density; g—gravity acceleration; D—the mantle thickness; k—thermal conductivity; $\kappa = k/\rho c_p$—thermal diffusivity; η—viscosity; and c_{p0} is thermal capacity.

For Cartesian models the values of Ra_{q} and Ra_{H} are the same, since $q = Q/S$ and $H = Q/(\rho DS)$, where Q is heat flow. However, Ra_{T} and Ra_{q} are different. They are related via Nusselt number (dimensionless heat flux):

$$\mathrm{Nu} = q/(\kappa \Delta T/D) = V_z T - dT/dz. \tag{2}$$

The Nusselt number is a direct measure of the convection intensity providing a relationship of the convection heat transport and

conduction. The relations (1) and (2) lead to:

$$Ra_q = Nu\, Ra_T. \tag{3}$$

We use these formulae to estimate effective parameters for the whole and upper mantle convection models. For the whole mantle model the mantle flux (q_m) is 72.4 mW m^{-2}; $D = 2900$ km; $g = 10$ m s^{-2}; $\rho = 4600$ kg m^{-3}; ($H = 9.23 \times 10^{-12}$ W kg^{-1}), $\alpha = 2 \times 10^{-5}$ K; $k = 5$ W m^{-1}; $\kappa = 10^{-6}$ m s^{-2} and $\eta = 2 \times 10^{21}$ Pa s (Schubert *et al.* 2001). Heat production in the core could be about 0.1 from internal heating, therefore the bottom heat flux is 2.5 less than the surface heat flux (Davies 1999). This gives the Rayleigh number $Ra_q \approx 5 \times 10^8$.

The upper mantle parameters are different: $\alpha = 3 \times 10^{-5}$ K^{-1}; $g = 10$ m s^{-2}; $\rho = 3600$ kg m^{-3}; $D = 700$ km, $k = 3.3 \approx 4$ W m^{-1}; $\kappa = 0.8 \approx 10^{-6}$ m s^{-2}; $\eta = 10^{21}$ Pa s; $q_m = 72.4$ mW m^{-2} (Schubert *et al.* 2001). Thus the Rayleigh number for the upper mantle is equal to $Ra_q \approx 4.8 \times 10^6$. The boundary layer theory and numerical calculations give a relation between the Rayleigh and Nusselt numbers $Nu \approx 0.2\, Ra_T^{1/3}$ (Schubert *et al.* 2001). Thus, $Ra_T \approx 3.2 \times 10^5$ and $Nu = Ra_q/Ra_T \approx 15$. For the reduced viscosity ($\eta = 5 \times 10^{20}$ Pa s) the Rayleigh number for upper mantle is equal to $Ra_q \approx 10^7$, $Nu \approx 18$ and $Ra_T \approx 6 \times 10^5$.

MODEL 1, WHOLE MANTLE CONVECTION

A. Parameters of the model, initial stage of the convection

Mantle convection is simulated in a 2-D ring (periodic boundary conditions) with the length to height ratio of 5:1. Calculations were performed for Rayleigh numbers $Ra_q = 5 \times 10^8$ ($Ra_T = 10^7$) implying internal and partially basal heating. We include only the most important phase transition at 660 km with the slope $dp/dT = -2$ MPa K^{-1} (Schubert *et al.* 2001). Viscosity η of the mantle depends on pressure p and temperature T. We use the simplified relationship suggested by Christensen (1984):

$$\eta(T, z) = A \exp[(-6.9T + 4.6(1 - z)], \tag{4}$$

where T—dimensionless (i.e. relative) temperature, and $1 - z$—dimensionless depth, A—constant scaling factor. According to eq. (4), the temperature and pressure variations in our model induce viscosity variations up to three and two orders of magnitude correspondingly.

The system of equations and boundary conditions are given in the Appendix. They are used to calculate evolution of the velocity and temperature patterns in the coupled system of the viscous mantle and floating rigid continents. Initially we take an arbitrary temperature distribution. After some period of heating, thermal convection is initiated in the box (Fig. 1, $t = 0$). Due to a temperature-dependent viscosity, the asthenosphere and lithosphere appear self-consistently as the low and high viscosity layers. Similar to other numerical models, the oceanic lithosphere is presented as the anomalously high viscous layer with variable thickness. It evolves in time, however, without disassembling into plates. For the Rayleigh number $Ra_q = 5 \times 10^8$ the convection pattern assumes a non-steady state motion. Periodical boundary conditions somewhat increase instability of the convection compared to the box with fixed sides.

Strong narrow downwellings simulate subduction zones (Fig. 1, $t = 0$). They can be traced through the entire mantle with some changes beneath the transition zone. The upwellings are generated at the bottom of the mantle. They are relatively narrow in the lower

mantle but in the upper mantle the upwellings become very wide (Fig. 1).

The calculated dimensionless heat flow (Nusselt number) as a function of depth and subadiabatic dimensionless temperature are shown in Fig. 2. For a non-steady convection $Nu(z)$ varies with time and has substantial depth fluctuations. Two $Nu(z)$ curves for different moments (0 and 20 Myr) are shown Fig. 2. The bottom dimensionless heat flux is $Nu_b \approx 12$ for the considered model. The surface Nusselt number is four times greater than the bottom one ($Nu_s \approx 50$).

Calculations are provided for dimensionless variables with the following scaling units: mantle thickness D for the distance; $V_0 = \kappa_0/D$ for the velocity; $t_0 = D^2/\kappa_0$ for the time. For the whole mantle model they are the follows $D = 2900$ km; $V_0 = 1.1 \times 10^{-3}$ cm yr^{-1}; $t_0 = 2.7 \times 10^{11}$ yr; $\eta_0 = 2 \times 10^{21}$. In the case of a quasi-steady state convection, maximal horizontal velocities (V_{xm}) are about 10^4. With the above scaling factor this gives $V_{xm} \approx 11$ cm yr^{-1}.

After initiation of mantle convection we instantaneously put a continent on the top. The continent (including the continental lithosphere) is modelled as a thick rigid flat body mechanically and thermally coupled with the mantle flow. Due to non-slip boundary conditions, mantle flow produces forces that include normal and shear stresses on the faces and bottom of the continent. Thermal coupling between the mantle and the continent is provided via boundary conditions (temperature and heat flux continuity). The continent consists of the main body ($l = 1.5$ in units of mantle thickness) and a small ($l = 0.05$) fragment. This fragment is used as a body marker for mantle velocities and demonstrates a possibility for detachment of some part of the continent at its active boundary. The thickness of the continent and its fragment is equal ($d = 0.1 \sim 300$ km). The initial temperature inside the thick continent is the same as it was in mantle at $t = 0$. Then, by solving the eq. (A8) (Appendix A) we calculate temperature variations inside the continent, which shows its thermal age.

We have tested the numerical code by comparing the results with available benchmarks. Without continents our results correspond to the benchmarks of Blankenbach *et al.* (1989). For the motionless (fixed) continent we find a good correspondence with Lowman & Jarvis (1999) and Bobrov *et al.* (1999). Thick floating continents coupled with the convecting mantle have not yet been considered and corresponding benchmarks simply do not exist. Therefore, to check a stability of our results we performed the calculations for a wide range of the initial parameters: density and size of the grid (80×200, 160×400 and 400×800), aspect ratio (5:1, 10:1) for the box and ring, thickness (d) and length (l) of the continent ($d = 0$ to 0.1 and $l = 0.05$ to 2), value of the Rayleigh number (from 10^5 to 10^9) and various initial positions of the continent. In all cases the obtained results show a qualitative similarity. In the following chapters we discuss only the effects, which appear in all models.

B. First stage of the evolution: formation of marginal basins

The continental plate with the small fragment is put on the top of convecting mantle (Fig. 1, $t = 0$). Several experiments have shown that the evolution of the mantle flow does not depend remarkably on the initial position of the continent. At the beginning, the continent moves together with its fragment. The velocity of the continent corresponds to the average mantle velocity at its bottom: $V_c \approx 1.8 \times 10^3 \approx 2.0$ cm yr^{-1}, which is about 0.2 of the maximal mantle flow velocity V_{xm}. Due to non-slip boundary conditions the mantle
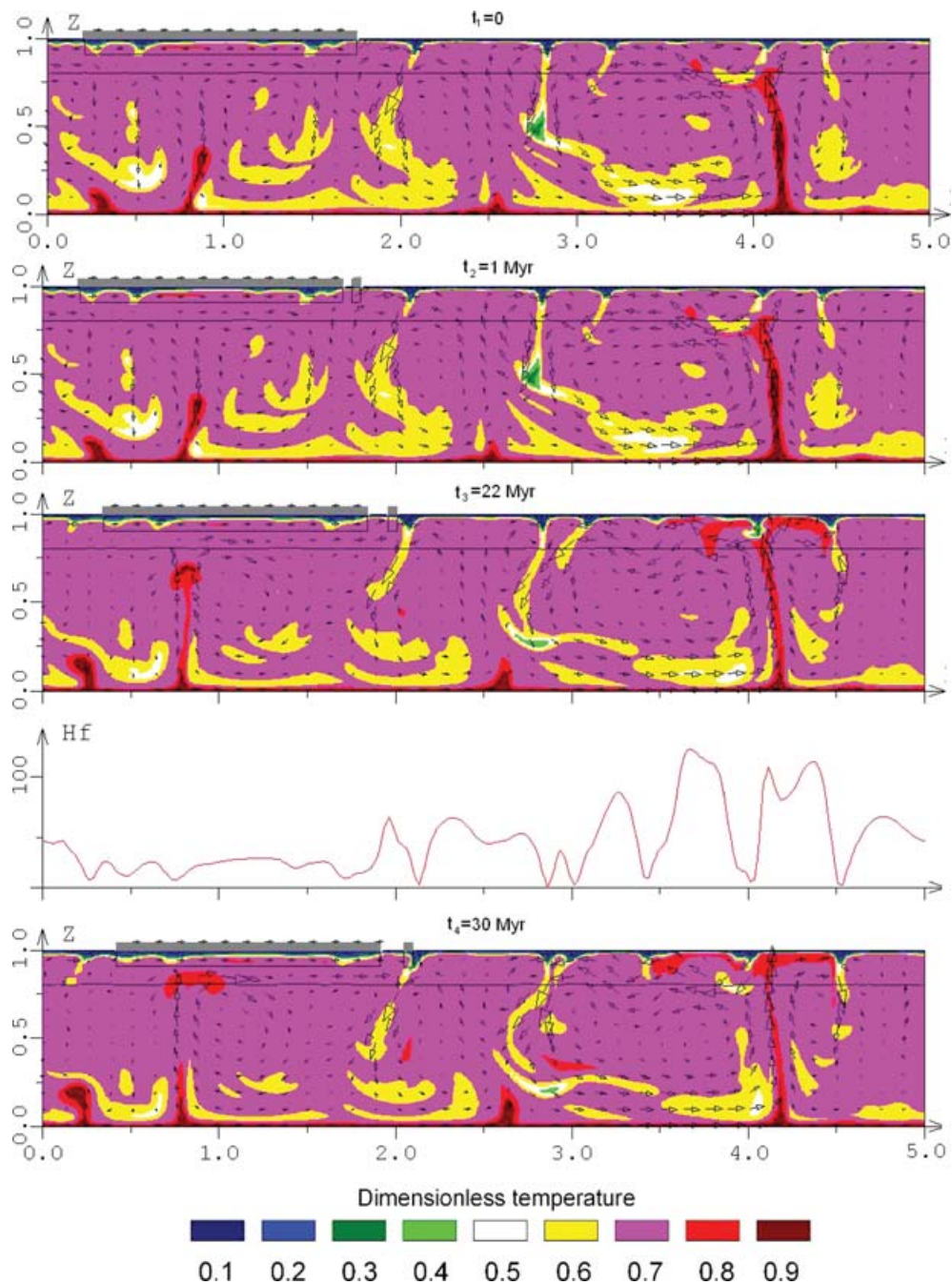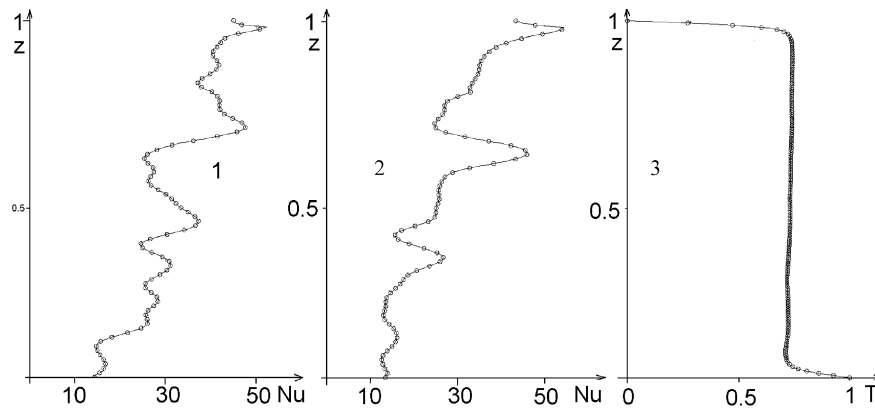
Figure 1. Whole mantle convection model. The first stage of the evolution of the model. Formation of marginal basins. Dimensionless subadiabatic temperature is shown in colour; the velocity vectors are indicated by arrows with maximal value $V_{xm} \approx 11$ cm yr^{-1}. Continent is shown in grey. Upper part of the continent (above mantle surface) is exaggerated. It is equal to 4 km and does not affect mantle convection. Red curve above the last pattern—surface dimensionless heat flow HF (Nusselt number). Phase boundary 660 km is shown by black line.

velocity near the bottom and faces of the continent become equal to the continental velocity.

Near-surface horizontal mantle velocity in the area between the continent and subduction zone varies significantly (Fig. 1). It is small near the continent due to non-slip conditions and also in the vicinity of the subduction zone because the total velocity vector turns down (the horizontal vector is zero on the top of subduction). As a result, the maximal horizontal velocity exists in the middle between the continent and subduction zone. Calculated at $t = 0$, the horizontal

mantle velocity $V_x(x)$ near the continent is equal to 1.8×10^3, and 3.5×10^3 in the middle area.

The fragment begins to separate from the continent at the moment, when the continental margin approaches a strong downwelling, where horizontal mantle flow velocities are much larger than the continental one (Fig. 1). Note, that this effect takes place due to a pull force of a downwelling, however, the role of upwellings is much smaller, since they are spread over a wide area in the upper mantle. At time $t_4 = 1.2 \times 10^{-4} = 30$ Myr the fragment is already close to

Figure 2. Whole mantle convection model. Calculated dimensionless heat flux Nu $(1 - z)$ as a function of depth $= (1 - z)$ for the time $t = 0$ (1) and $t = 20$ Myr (2). (3)—temperature variation with depth. z-distance from the bottom. All parameters are horizontally averaged.

the downwelling and its horizontal velocity becomes approximately the same as of the continent ($V_c \approx V_f \approx 1.9 \times 10^3 \approx 2.1$ cm yr^{-1}).

This structure near the continental margin is similar to a typical marginal basin. A local maximum of the calculated heat flux appears in between the continent and its fragment. The horizontal deviatoric stress $\tau_{xx} = 2\eta(\partial V_x/\partial x)$ is positive (extension) in the part of the marginal basin near the continent. It leads to a stretching of the oceanic lithosphere, which is defined as a thermal boundary layer with mostly conductive heat transport (Schubert *et al.* 2001). Near the subduction zone, where the horizontal velocity decreases, the deviator stress is negative and the oceanic lithosphere becomes thick.

C. Second stage of the evolution: closing of marginal basin

Fig. 3 shows next period of the mantle–continent evolution. The continent continues to move towards the downwelling. At time $t_5 = 2.8 \times 10^{-4} \approx 75$ Myr the calculated velocities of the continent and fragment are equal to $1.6 \times 10^3 \approx 1.8$ cm yr^{-1}, $V_f \approx 1.2 \times 10^3 \approx 1.3$ cm yr^{-1} respectively. At time $t_7 = 5 \times 10^{-4} = 135$ Myr the continent achieves the fragment and they move with the identical velocity $V_f \approx 1.35 \times 10^3 \approx 1.5$ cm yr^{-1}. As a result the marginal basin disappears.

It is important to note that during the considered time period of evolution the subduction zone does not stand in one place but also moves. As it can be seen from Fig. 3, at the time period $t_7 - t_5 = 2.2 \times 10^{-4} = 60$ Myr the subduction has been shifted towards ocean for the distance of about $\Delta x = x_7 - x_5 = 0.3 = 900$ km, which gives the mean roll-back velocity of about $V_{sub} \approx 1.3$ cm yr^{-1}.

Comparing Figs 1 and 3 one may realize, that after about 100 Myr the mantle becomes warmer. This is the result of a continent insulation effect. Mantle heat can penetrate through the continent only by conduction. As a result the mantle flux over the continent is three to four times less than over the ocean. The modelled continent covers approximately one-third of the mantle surface and the insulation leads to mantle warming. Consequently the temperature under the continent excluding the uppermost part is increased even in the lower mantle. At the same time the continental lithosphere becomes cooler and thicker due to near zero vertical velocities and consequently low heat transport in the uppermost mantle.

The mantle currents at the bottom of the continent force it to move to the right. The oceanic lithosphere generally moves in opposite direction. As a result, after closing of the marginal basin the

extension regime is replaced by compression and the large horizontal stress $\tau_{xx} = 2\eta\,(\partial V_x/\partial x)$ must appear at the active boundary of the continent.

### MODEL 2, UPPER MANTLE CONVECTION: THREE STAGES OF THE CONTINENT–MANTLE SYSTEM EVOLUTION

To investigate specific effects that appear in the upper mantle (e.g. from narrow upwellings), we consider another model with parameters appropriate for layered upper mantle convection (Schubert *et al.* 2001). We explore the ring model with an aspect ratio of 5:1 (with periodical boundary conditions), but with basal heating only and with the temperature Rayleigh number $Ra_T = 10^6$. Scaling units for this model are as follows: $D = 700$ km; $V_0 = 4.5 \times 10^{-3}$ cm yr^{-1}; $t_0 = 1.6 \times 10^{10}$ yr. Again, viscosity is controlled by pressure and temperature:

$$\eta = 7 \times 10^{21} \times \exp[(-4.6T + 0.92(1 - z)]. \tag{5}$$

The distributions of the heat flux $Nu(z)$, temperature and viscosity with depth (horizontally averaged) are shown in Fig. 4. The convection pattern is in a quasi-steady state and the Nusselt number $Nu(z)$ almost does not vary with depth (Nu ≈ 18). The corresponding heat flux Rayleigh number is $Ra_q = Nu \times Ra_T \approx 2 \times 10^7$. The lithosphere and asthenosphere appear in the upper mantle as high and low viscosity layers (Fig. 4). The mean mantle viscosity is $\eta = 5 \times 10^{20}$, the maximal mantle velocity is equal to $V_m \approx 600 \approx 2.7$ cm yr^{-1}.

A. First stage: continent slowly moves towards a downwelling

At time, set as zero, a rigid continent is placed on top of the mantle as shown in Fig. 5. Similar to previous model the continent is modelled as a rigid composite flat body consisting of the main part ($l = 1.5$) and a small ($l = 0.05$) fragment. The initial thickness of the continent ($d = 0.05$) is less than in the whole mantle model, since in this case we are also going to model the process of lithosphere formation. Initially we assume the same temperature distribution within the continent as in the mantle material the continent has replaced (Fig. 5, $t = 0$). Then the mantle–continent system evolves in time together with the temperature distribution and is calculated
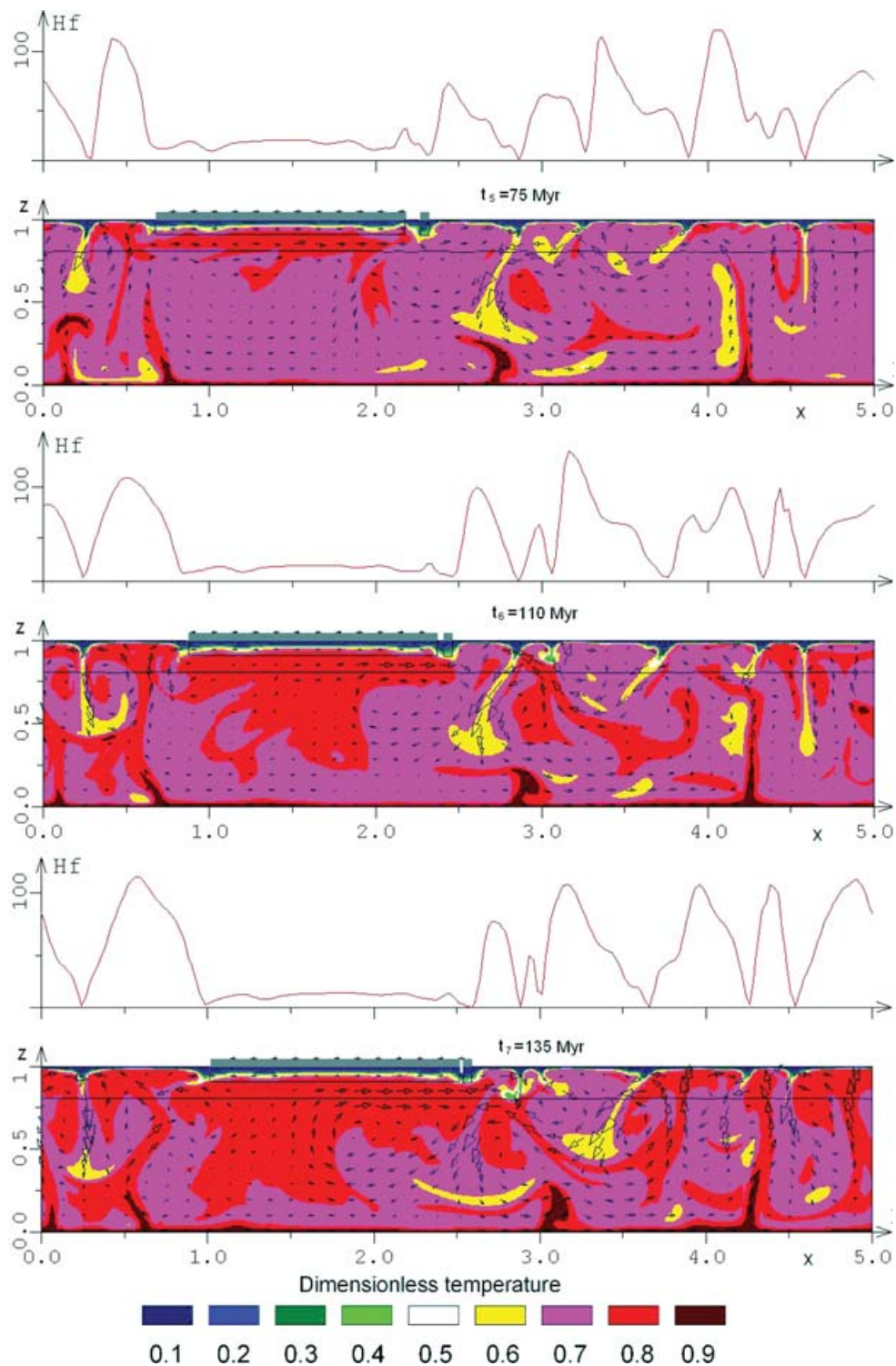
Figure 3. Whole mantle convection model. The same as in Fig. 1, but for the second stage of the continental evolution: closing of the marginal basin.

self-consistently using eq. (A8) coupled with eqs (A1)–(A9) (see Appendix).

The first stage is shown in Fig. 5. The velocity of the continent is equal to the average mantle velocity at the bottom of the continent and is $v \approx 60 \approx 0.3$ cm yr^{-1}, which is about 0.1 of the maximal mantle flow velocity. Over $t_2 = 1 \times 10^{-4} = 1.6$ Myr the continent moves slowly towards a downwelling (Fig. 5, t_2). Repeating the whole mantle scenario, the mantle drag pulls the continental frag-

ment since the mantle velocity under the continental edge is much higher than the velocity of the continent. As a result the oceanic lithosphere near the edge is stretched and becomes thin. At $t_2 = 1.6$ Myr and $t_3 = 13$ Myr, the small detached fragment has moved away from the continent, towards the subduction zone (Fig. 5, t_2 and t_3). From Fig. 5 ($t_4 = 1 \times 10^{-3} = 16$ Myr) one can see that an inclined subduction zone appears self-consistently without applying any predefined stresses or velocities. The small continental
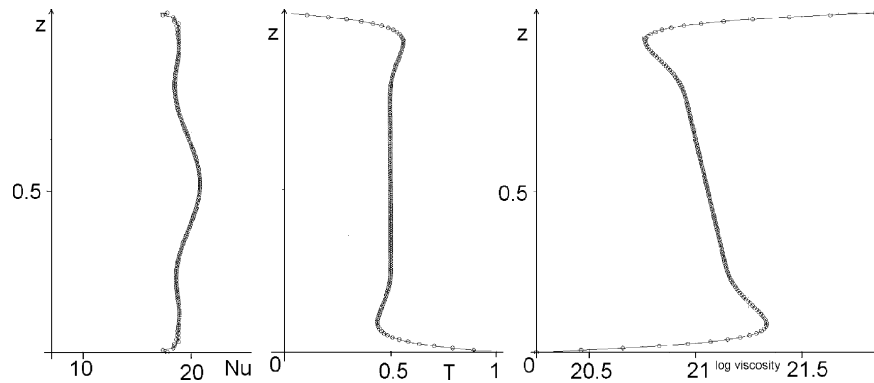
Figure 4. Upper mantle model. Calculated distributions of the heat flux $Nu(1 - z)$, dimensionless temperature $T(1 - z)$ and viscosity $h(1 - z)$. z-distance from the bottom, $1 - z$ depth. All parameters are horizontally averaged.

fragment sits above the downwelling at the top of subduction zone, which behaves like a trap.

B. Second stage: marginal basin closes and the continent overrides the subduction zone

The next stage of the evolution is shown in Fig. 6. During the time period $t_5 - t_7$ the continent continues to move towards the subduction zone with the mean velocity of about $V_s \approx 550 \approx 2.5$ cm yr^{-1}. On the other hand, the subduction zone also moves together with the continental fragment in the same direction, although with less velocity ($V_f \approx 330 \approx 1.4$ cm yr^{-1}). Therefore, a roll back of subduction appears self-consistently also in the upper mantle model. At time $t_8 = 1.8 \times 10^{-3} \approx 29$ Myr the moving continent reaches the subduction zone and the marginal basin closes. At this moment the extension regime is replaced by strong compression and the continental fragment is re-attached to the continent. The compression might be expected to cause active mountain building.

Due to roll back, the distance between the upwelling and the subduction zone is reduced and the ocean in the front of the continent becomes non-symmetrical: the distance between the continent and the upwelling is several times less than between the upwelling and the downwelling (subduction) on the right side, Fig. 6.

Over 30 Myr the continent (especially the deeper continental lithosphere) becomes remarkably colder. It makes continental lithosphere more viscous, strong and consequently stable. The model also demonstrates possible detachment of the lithospheric slab, which is then transported to the bottom, Fig. 6, $t_5 \approx 19$ Myr.

C. Third stage: continent overrides upwelling

At time $t_{10} \approx 35$ Myr the moving continent reaches the upwelling as it is shown in Fig. 7. Then at $t_{11} \approx 37$ Myr the continent partially overrides the upwelling that is now close to the downwelling. Subduction in its classical form stops. Due to the hot upwelling material, temperature under and inside the right edge of the continent increases, Fig. 7 ($t_{12} \approx 42$ Myr). This effect decreases the both viscosity and the thickness of the continental lithosphere.

DISCUSSION

During the last three decades many attempts were made to explain the origin of marginal basins (e.g. Karig 1971; Chase 1978; Hsui & Toksoz 1981; Taylor & Karner 1983; Hynes & Mott 1985; Jarrard 1986; DeMets 1992). It has been proposed that there exist basically

two types of subduction zones (Uyeda & Kanamori 1979; Nakamura & Uyeda 1980): If the adjacent continent is being driven against the trench, as in Chili, marginal basins do not develop. If the adjacent continent is stationary relative to the trench, as in the Marianas, the weakening of the lithosphere leads to a series of marginal basins as the trench migrates seawards (Schubert *et al.* 2001).

The results of our modelling show that these two types of active continental margins logically represent different stages of the continental evolution. As it was mentioned above, the velocity of a continent is several times lower than the maximal oceanic plate velocity (e.g. halfway between the velocity of an upwelling and a subduction zone). Near a subduction zone the mantle flow becomes almost vertical. Thus, the horizontal mantle flow velocity under the continental edge depends on the position of a continent relative to down and upwelling, also controlling the stress state (compressional or extensional). These modelling results might explain the origin of some marginal basins at the active boundary of Eurasia. The findings agree with geological reconstructions (Maruyama 1997; Maruyama *et al.* 1997), which show that Japan islands divided from Eurasia about 20 Myr ago. This model represents a new look on the marginal basins' origin compared to the previous models (e.g. Schubert *et al.* 2001). It could explain the observable data on the stress patterns within marginal basins (Jarrard 1986): extension near the continental edge and compression close to the subduction. This calculated stress state in marginal basin is in accordance with observable data (Jarrard 1986). Our modelling self-consistently reveals that local maximum of heat flux in marginal basin is connected with stretching and thinning of lithosphere (Figs 1 and 5).

All our models reveal also a second stage of mantle system evolution. When the continental fragment set over a downwelling, it continues to move with it as in a trap. However, the continent moves faster and, despite the roll back, after some time it overruns down the fragment. The duration of this stage is very sensitive to the model parameters, particularly viscosity. When the continent reaches the subduction zone, the extension regime at the continental edge is replaced by strong compression. These stresses may initiate fast mountain building, like at the western edge of South America.

At the third stage of the evolution the continent overrides the upwelling and subduction in its classical form stops. This process is similar to the evolution of Western North America. The third stage appears only in the upper mantle (i.e. layered) convection model. We could not reproduce it in the model with the parameters of whole mantle convection. The whole mantle model distinctly shows subduction zones but does not reveal localized upwellings,
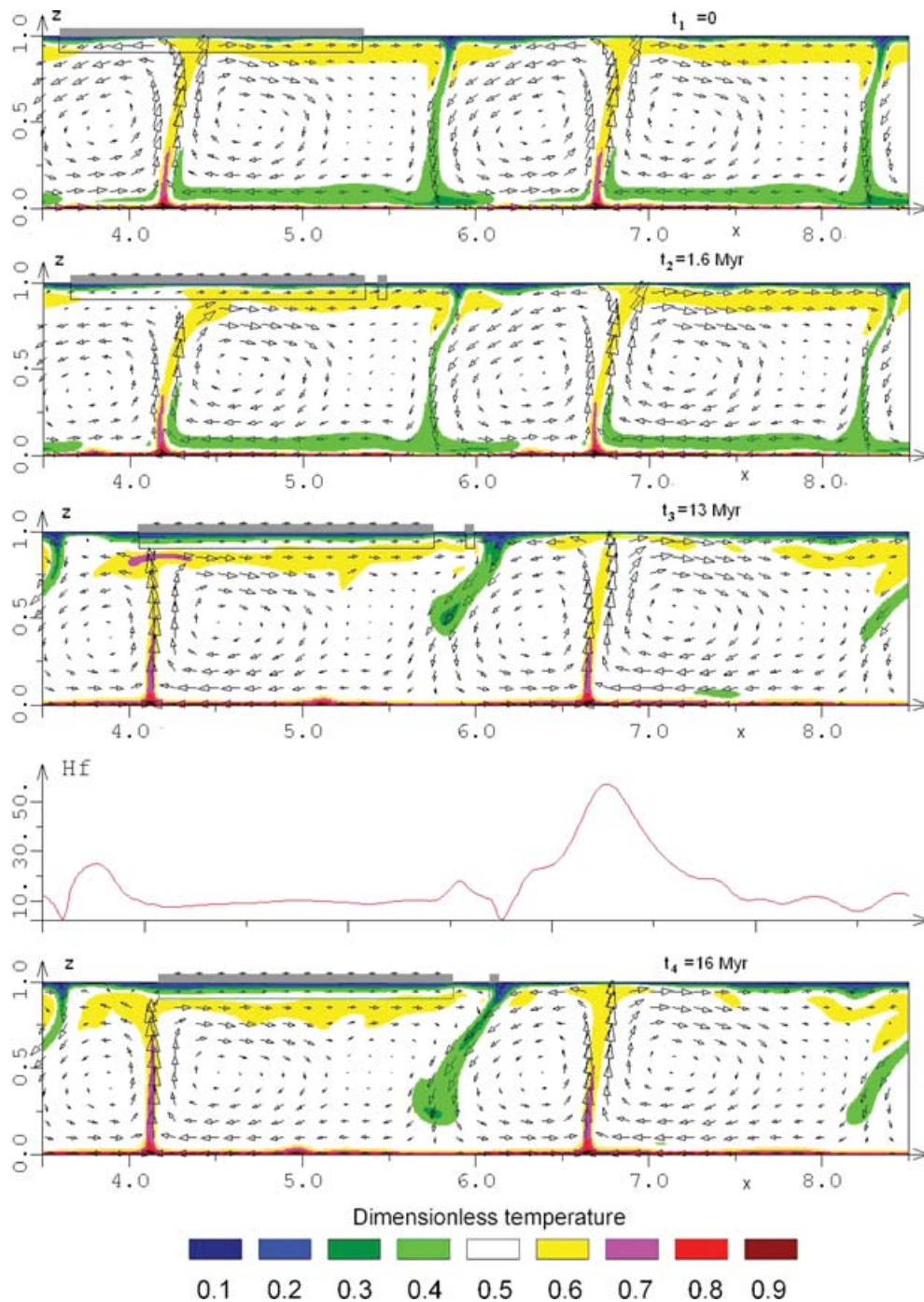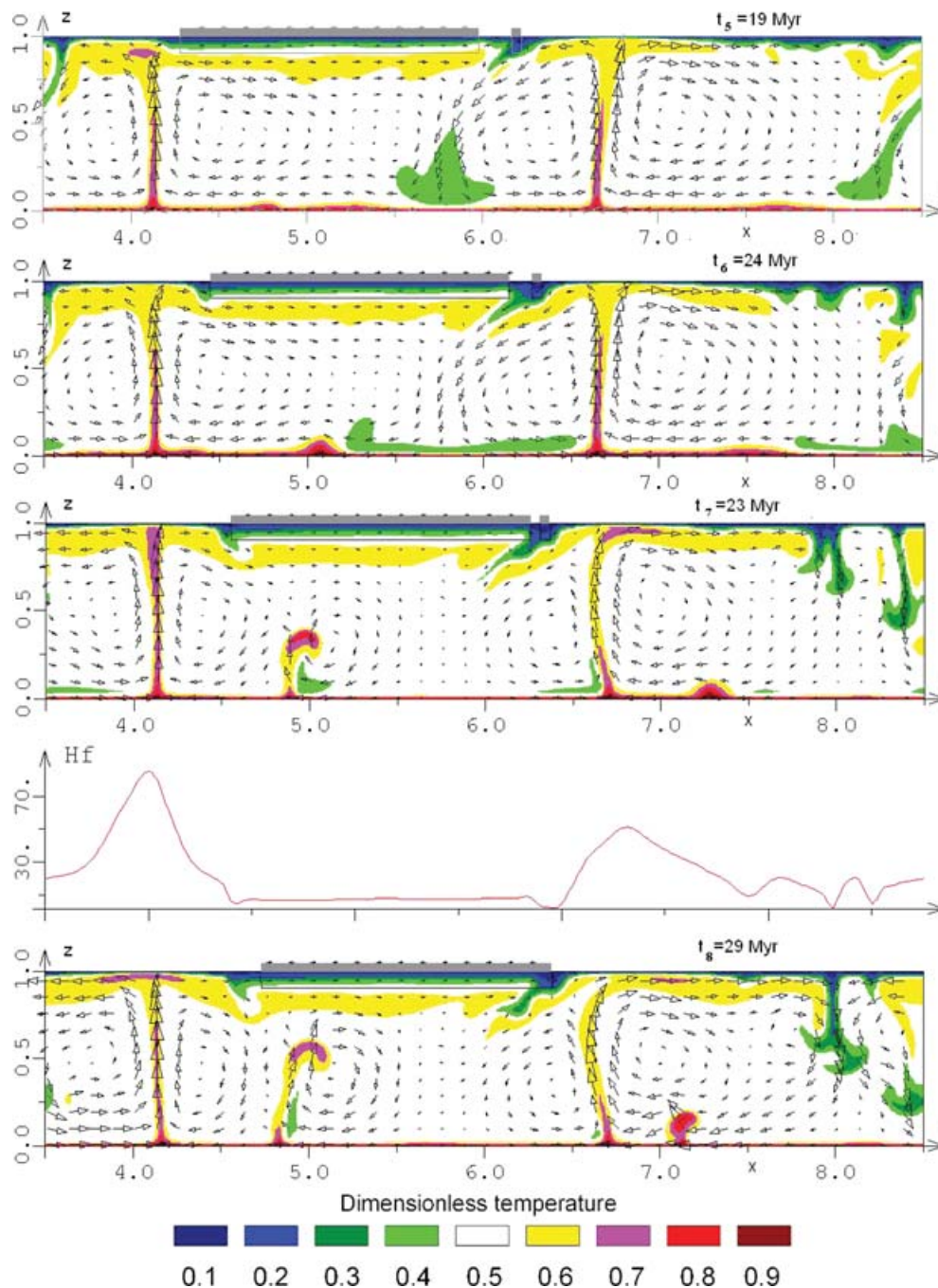
Figure 5. Upper mantle model. First stage of the continent–mantle evolution: opening of marginal basin. The legend is the same as in Fig. 1. Maximal mantle flow velocity corresponds to 2.7 cm yr^{-1} (see text).

which play a principal role in the third phase. A comprehensive model, which might self-consistently explain the appearance of mid-oceanic ridges, should imply solid oceanic lithosphere. Development of such a model that explains the interaction of the system of oceanic plates with convection flows, even without continents, is in a very initial stage (Tackley 2000a,b; Zhong *et al.* 2000; Bercovici 2003). Instead, it is suggested here to use a simplified model with the parameters of upper mantle convection. It is clear that the local-ized upwellings, which appear in the upper mantle model, may not be considered as full analogues of mid-oceanic ridges representing rather passive than active structures. Therefore, we consider the fi-

nal stage of the model evolution as a very first approximation of real upper mantle–lithosphere processes.

This model reveals three stages of evolution for various values of viscosity, sizes of continent and Rayleigh numbers. The roll back of the subduction zone still continues after closure of the marginal basin and the continent moves towards the upwelling. However, the continent does not affect the subduction zone on the opposite side of the ridge (in a reality the continent may be just small). As a result, a non-symmetric ocean structure appears. Such situation resembles some features the present-day South Pacific. This effect appears in all models (e.g. with various Rayleigh numbers) and

Figure 6. Upper mantle model. Second stage of the continent–mantle system evolution: back-rolling and closing of marginal basin. The legend is the same as in Figs 1 and 5.

does not result from a 'wall' effect (this appears also with periodic ring conditions). When the continent achieves the upwelling and overrides it, subduction (in its classical case) is terminated. This situation is principally different from the convection models without continent, in which the up and downwellings are spaced apart by a distance equal to the length of a convection cell.

CONCLUSIONS

The numerical modelling of the mantle–continent system reveals several regularities of its evolution that do not depend critically on

the model parameters. It is demonstrated that downwellings play a dominant role not only in mantle dynamics but also in deforming continental motion. Mechanical and thermal interaction of mantle convection and thick floating continent leads to substantial changes of the stresses in the mantle near the leading edge of a moving continent.

Our model reveals self-consistently several principal stages of continental evolution that occurred after the break-up of Pangea. Palaeomagnetic reconstructions show that continents separated from one supercontinent at different times and started to move with different velocities. As a result, the continents are presently at
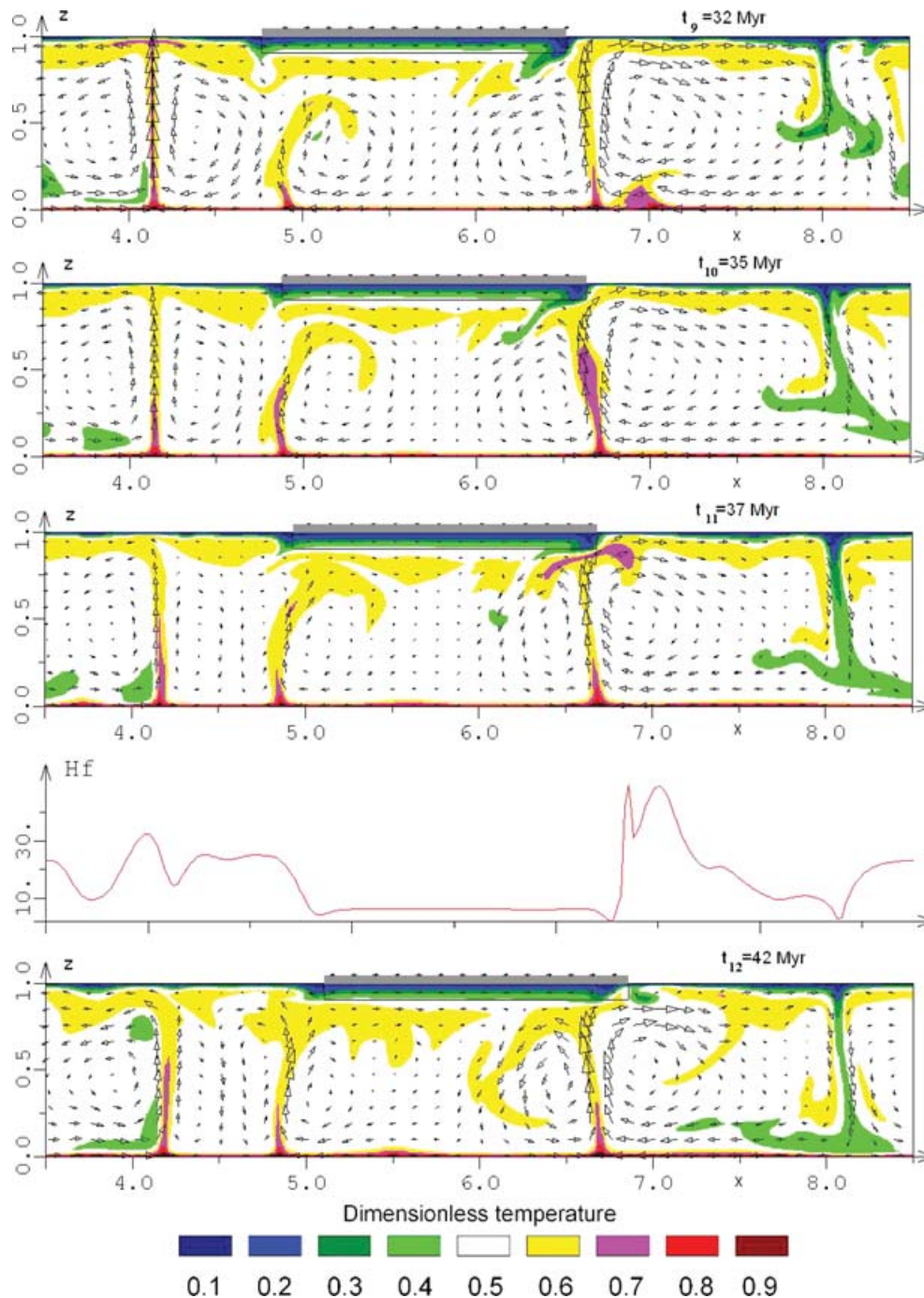
Figure 7. Upper mantle model. Third stage of the continent–mantle system evolution: continent overrides mid-oceanic ridge. The moving continent reaches the upwelling (ridge crest). Subduction in its classical form stops, and the right boundary of continental lithosphere becomes warm. The legend is the same as in Figs 1 and 5.

different stages of their evolution. North America split first and moved fast from the very beginning. Thus, North America has already passed through the initial stages and attained the third stage, when a mid-ocean ridge goes under the western continental boundary and typical subduction stops. Following North America, South America has separated from Pangea. At present, South America is in the second stage of the continental evolution with a compression regime at the active boundary, which leads to the mountain belt formation (Andes) and the subduction zone just under the continental boundary. These results could explain the trenches' migration at

the western margins of North and South America (Morgan 1983; Zhong & Gurnis 1995). Eurasia was assembled from some shields just before the formation of Pangea. After the break-up of Pangea, Eurasia began to move only later in time and is presently in the initial evolutionary stage with an extension regime near its leading boundary. The inclined subduction zone appears self-consistently in the first numerical model without predefining velocities or stresses. At this stage the subduction zone is separated from the continent by the backarc marginal basin that is characterized by a high heat flow.

Despite the fact that the main results presented here are robust relative to the model parameters, they should be considered as qualitative ones. The numerical models used here are simplified and can reveal only general tendencies of continental evolution. The calculated quantitative values of velocities and time durations are sensitive to initial conditions and prehistory of mantle–continent system. The real continental evolution is much more complicated than described here. Further development of the model needs to focus on inclusion of high viscosity oceanic plates and improving the mantle convection models.

ACKNOWLEDGMENTS

REFERENCES

Arnold, J., Jacoby, W.R., Schmeling, H. & Schott, B., 2001. Continental collision and the dynamic and thermal evolution of the Variscan orogenic crust root—numerical models, *J. Geodyn.,* **31,** 273–291.

Bercovici, D., 2003. The generation of plate tectonics from mantle convection, *Earth planet. Sci. Lett.,* **205,** 107–121.

Blankenbach, B. et al, 1989. A benchmark comparison for convection codes, *Geophys. J. Int.,* **98,** 23–38.

Bobrov, A.M., Jacoby, W. & Trubitsyn, V.P., 1999. Effects of Rayleigh number, length and thickness of continent on time of mantle flow reversal, *J. Geodyn.,* **27,** 133–145.

Chase, C.G., 1978. Extension behind island arcs and motion relative to hot spots, *J. geophys. Res.,* **83,** 5385–5387.

Christensen, U.R., 1984. Heat transport by variable viscosity convection for the Earth's thermal evolution, *Phys. Earth planet. Inter.,* **35,** 264–282.

Christensen, U.R. & Yuen, D.A., 1984. The interaction of a subducting lithospheric slab with a chemical or phase boundary, *J. geophys. Res.,* **89,** 4389–4402.

Christensen, U.R. & Yuen, D.A., 1985. Layered convection induced by phase transition, *J. geophys. Res.,* **90,** 10 291–10 300.

Condie, K.C., 1998. Episodic continental grouth and supercontinents: a mantle avalanche connection?, *Earth planet. Sci. Lett.,* **163,** 97–108.

Davies G.F., 1988. Role of the lithosphere in mantle, *J. geophys. Res.,* **93,** 10 451–10 466.

Davies, G.F., 1999. *Dynamic Earth, Plates, Plumes and Mantle Convection,* Cambridge University Press, Cambridge, p. 458.

Duncan, C.C. & Turcotte, D.L., 1994. On the breakup and coalescence of continents, *Geology,* **22,** 103–106.

DeMets, C., 1992. A test of present-day plate geometries for Northeast Asia and Japan, *J. geophys. Res.,* **97,** 17 627–17 635.

Gable, C.W., O'Connell, R.J. & Travis, B.J., 1991. Convection in three dimensions with surface plates: Generation of toroidal flow, *J. geophys. Res.,* **96,** 8391–8405.

Griffin, W.L. *et al*., 1999. Layered mantle lithosphere in the Lac de Gras Area, Slave Craton: composition, structure and origin, *J. Petrol.,* **40,** 705–727.

Gurnis, M., 1988. Large-scale mantle convection and aggregation and dispersal of supercontinents, *Nature,* **332,** 696–699.

Gurnis, M. & Zhong, S., 1991. Generation of long wavelength heterogeneities in the mantle dynamics interaction between plates and convection, *Geophys. Res. Lett.,* **18,** 581–584.

Hsui, A.T. & Toksoz, M.N., 1981. Back-arc spreading: trench migration, continental pull or induced convection?, *Tectonophysics,* **74,** 89–98.

Hynes, A. & Mott, J., 1985. On the causes of back-arc spreading, *Geology,* **13,** 387–389.

Jarrard, R.D., 1986. Relations among subduction parameters, *Rev. Geophys.,* **24,** 217–284.

Jordan, T.H., 1978. Composition and development of the continental tectosphere, *Nature,* **274,** 544–548.

Kaban, M.K., Schwintzer, P., Artemieva, I.M. & Mooney, W.D., 2003. Density of the continental roots: compositional and thermal contributions, *Earth planet. Sci. Lett.,* **209,** 53–69.

Karig, D.E., 1971. Origin and development of marginal basins in the west Pacific, *J. geophys. Res.,* **76,** 2542–2561.

King, S.D., Gable, C.W. & Weinstein, S.A., 1992. Model of convection-driven tectonic plate: a comparison of methods and results, *Geophys. J. Int.,* **109,** 481–487.

King, S.D. & Ritsema, J., 2000. African hot spot volcanism: small-scale convection in the upper mantle beneath cratons, *Science,* **290,** 1137–1140.

Lenardic, A. & Kaula, W.M., 1995. Mantle dynamics and the heat flow into the Earth's continents, *Nature,* **378,** 709–711.

Lenardic, A. & Moresi, L.-N., 1999. Some thought on stability cratonic lithosphere: effects of buoyancy and viscosity, *J. geophys. Res.,* **104,** 12 747–12 758.

Lowman, J.P. & Jarvis, J.T., 1995. Mantle convection models of continental collision and breakup incorporating finite thickness plates, *Phys. Earth planet. Inter.,* **88,** 53–68.

Lowman, J.P. & Jarvis, J.T., 1999. Effects of mantle heat source distribution on supercontinent stability, *J. geophys. Res.,* **104,** 12 733–12 746.

Marquart, G., Schmeling, H., Ito, G. & Schott, B., 2000. Condition for plumes to penetrate the mantle phase boundaries, *J. geophys. Res.,* **105**(3), 5679–5693.

Maruyama, S., 1997. Pacific-type orogeny revised: Miyashiro-type orogeny proposed, *The Islands Arc.,* **6**(1), 91–120.

Maruyama, S., Isozaki, Y., Kimura, G. & Terabayashi, M., 1997. Paleogeographic maps of the Japanese islands: plate tectonic synthesis from 750 Ma to present, *The Islands Arc.,* **6**(1), 121–142.

Morgan, J.W., 1983. Hotspot tracks and opening of the Atlantic, *Tectonophysics,* **94,** 123–129.

Nakamura, K. & Uyeda, S., 1980. Stress gradient in arc-back arc regions and plate subduction. *J. geophys. Res.,* **85,** 6419–6428.

Olson, P. & Corcos, G.M., 1980. A boundary layer model for mantle convection with surface plates, *Geophys. J. R. astr. Soc.,* **62,** 195–219.

Richter, F.M., 1973. Finite amplitude convection through a phase boundary, *J. R. Astron. Soc.,* **35,** 265–276.

Ritsema, J. & van Heijst, H.J., 2000. Seismic imaging of structural heterogeneity in Earth's mantle: evidence for large-scale mantle flow, *Science Progress,* **83,** 243–259.

Schott, B., Yuen, D.A. & Schmeling, H., 2000. The diversity of tectonics from fluid-dynamical modeling of the lithosphere-mantle system, *Tectonophysics,* **322**(1–2), 35–51.

Schubert, G., Turcotte, D.L. & Olson, P., 2001, *Mantle Convection in the Earth and Planets*, Cambridge University Press, Cambridge, p. 940.

Stein, M. & Hofmann, A.W., 1994. Mantle plumes and episodic crustal growth, *Nature,* **372,** 63–68.

Tackley, P.J., 2000a. Self-consistent generation of tectonic plates in time-dependant, three-dimensional mantle convection simulations, 1, Pseudoplastic yielding, *Geochem. Geophys. Geosyst.,* Vol. 1, Paper number: 2000G000036.

Tackley, P.J., 2000b. Self-consistent generation of tectonic plates in time-dependant, three-dimensional mantle convection simulations, 2, Strain weakening and asthenosphere, *Geochem. Geophys. Geosyst.,* Vol. 1, Paper number: 2000G000043.

Taylor, B. & Karner, G.D., 1983. On the evolution of marginal basins, *Rev. Geophys,* **21,** 1727–1741.

Toksoz, M.N. & Hsui, A.T., 1978. Numerical studies of back-arc and the formation marginal basin, *Tectonophysics,* **50,** 177–196.

Trubitsyn, V.P. & Rykov, V.V., 1995. A 3-D Numerical Model of the Wilson Cycle, *J. Geodyn.,* **20,** 63–75.

Trubitsyn, V.P., Rykov, V.V. & Jacoby, W., 1999. A self-consistent 2-D model for the dip angle of mantle downflow beneath an overriding continent, *J. Geodyn.* **28,** 215–224.

Trubitsyn, V.P. & Rykov, V.V., 2000. 3-D spherical models of mantle convection with floating continents, U.S. Geological Survey Open File Report 00-218, pp. 2-44.

Trubitsyn, V.P., 2000a. Phase transitions, compressibility, thermal expansion and adiabatic temperature in the mantle, Izvestiya, *Physics of the Solid Earth,* **36,** 101–113.

Trubitsyn, V.P., 2000b. Principles of the tectonics of floating continents, Izvestiya, *Physics of the Solid Earth,* **36,** 708–741.

Trubitsyn, V.P., Mooney, W.D. & Abbott, D.H., 2003. Cold cratonic roots and thermal blankets: how continents effect mantle convection, *International Geology Review,* **45,** 479–496.

Turcotte, D.L. & Schubert, G., 1982. *Geodynamics: Applications of Continuum Physics in Geological Problems,* John Wiley, New York, 450 p.

Uyeda, D. & Kanamori, H., 1979. Back-arc opening and the mode of subduction, *J. geophys. Res.,* **84,** 1049–1061.

Yuen, D.A., Reuteler, D.M., Balanchandar, S., Steibach, V., Malevsky, A.V. & Smedmo, J.J., 1994. Various influences on the three-dimension mantle convection with phase transition, *Phys. Earth planet Int.,* **86,** 185–203.

Nakakuki, T., Yuen, D.A. & Honda, S., 1997. The interaction of plumes with the transition zone under continents and oceans, *Earth planet. Sci. Lett.,* **146,** 379–391.

Zalesak, S.T., 1979. Fully multidimensional flux-corrected transport algorithms for Fluids, *J. Comput. Phys.,* **31,** 335–361.

Zhong, S. & Gurnis, M., 1993. Dynamic feedback between a continentlike raft and thermal convection, *J. geophys. Res.,* **98,** 12 219–12 232.

Zhong, S. & Gurnis, M., 1995. Mantle convection with plates and mobile, faulted plate margins, *Science,* **267,** 838–843.

Zhong, S., Zuber, M.T., Moresi, L. & Gurnis, M., 2000. Role of temperature-dependent viscosity and surface plates in spherical shell models of mantle convection, *J. geophys. Res.,* **105,** 11 063–11 082.

APPENDIX

Mantle convection coupled with floating continents is modelled using classical Stokes' equations for viscous flow and the equations to describe motion of a floating rigid body. Viscosity of the mantle is variable, phase transition may also be implemented in the model. A rigid continent is submerged in the convecting mantle like an iceberg, it is coupled with the mantle via boundary conditions, which assume all thermal and mechanical interactions at the interface. The numerical code is based on the model introduced in Trubitsyn (2000b). Results for mantle convection without continent have been verified using the benchmark from Blankenbach *et al.* (1989).

A. Equations of thermal convection

Thermal convection for the 2-D model is described by Stokes equations, the equation of heat transfer and the equation of continuity with variable parameters (*cf.* Schubert *et al.* 2001). In Boussinesq approximation the latent effect of phase transformations can be neglected, because the thermal effect of phase transformation is smaller than their buoyancy effect (Christensen & Yuen 1984):

$$-\partial p/\partial x + \partial[\eta(\partial V_x/\partial z + \partial V_z/\partial x)]/\partial z + 2\partial(\eta \partial V_x/\partial x)/\partial x = 0, \tag{A1}$$

$$-\partial p/\partial z + \partial[\eta(\partial V_z/\partial x + \partial V_x/\partial z)]/\partial x$$
$$+ 2\partial(\eta \partial V_z/\partial z)/\partial z + Ra_T T - R_b \Gamma = 0, \tag{A2}$$

$$\partial T/\partial t + V_x \partial T/\partial x + V_z \partial T/\partial z = \partial/\partial x(\kappa \partial T/\partial x)$$
$$+ \partial/\partial z(\kappa \partial T/\partial z) + H, \tag{A3}$$

$$\partial V_x/\partial x + \partial V_z/\partial z = 0, \tag{A4}$$

where V_x and V_z, p and T are dimensionless components of velocity, pressure and temperature respectively, and H is internal heat production; Γ is phase function (Richter 1973; Christensen & Yuen 1984). As usual, eqs (A1)–(A4) are given in dimensionless form. Corresponding scaling parameters are listed above in the main text. The thermal Rayleigh number Ra_T and the phase Rayleigh number are equal to:

$$Ra_T = \alpha_0 \rho g \Delta T D^3/(\kappa_0 \eta_0), \quad R_b = g \Delta \rho D^3/(\kappa_0 \eta_0), \tag{A5}$$

where g is gravity acceleration, ρ is density and $\Delta \rho$ is phase density jump. Phase function Γ can be written in the simple form $\Gamma(\xi) = 1/[1 + \exp(-4\xi)]$ with $\xi(h, T) = [h - h* + \gamma(T - T^*)]/\delta h$, where Γ is phase slope and δh is the thickness of phase transition zone (Schubert *et al.* 2001; Trubitsyn 2000a).

Eqs (A1)–(A3) can also be used with phase transitions in the mantle, which could be included by means of generalized effective parameters α, c_p, and compressibility $1/K$. The phase transition is modelled as a delta function, representing sharp changes of the parameters in the transition zone (Christensen & Yuen 1985; Yuen *et al.* 1994; Trubitsyn 2000a; Schubert *et al.* 2001).

B. Equations for floating continent

Since we assume that the continent is a rigid floating body, the velocity of each point of this body is equal to the velocity at the centre of gravity $u_x(x, z) = u_0$, assuming that vertical velocities are close to zero: $u_z(x, z) = 0$. The continent is driven by the forces originated from the mantle flow. The total mantle force moving the continent represents a sum of the ridge-push and slab-pull forces on its faces and the mantle-drag force on its bottom (Trubitsyn *et al.* 1999; Trubitsyn & Rykov 2000):

$$m \partial u_0/\partial t = \int_{1-d}^{1} [(p)_{x=x_1} - 2\eta(\partial V_x/\partial x)_{x=x_1}]\, dz$$
$$- \int_{1-d}^{1} [(p)_{x=x_2} - 2\eta(\partial V_x/\partial x)_{x=x_2}]\, dz$$
$$- \int_{x_1}^{x_2} \eta[(\partial V_x/\partial z)_{z=1-d} + (\partial V_z/\partial x)_{z=1-d}]\, dx, \tag{A6}$$

where m is a dimensionless mass of the continental plate per unit length, d and l are the thickness and length of the plugged part of the continent, and $x_1(t)$ and $x_2(t) = x_1(t) + l$ are the coordinates of its left and right corners, satisfying the condition:

$$dx_1/dt = u_0. \tag{A7}$$

The left-hand side of eq. (6) (acceleration of the continent) is small and is set to zero.

The equation for the temperature $T_c(x, z)$ inside the continent (in the original coordinate system) is the heat conduction equation incorporating internal heat production (H_c) with the advective transfer term:

$$\partial T_c/\partial t + u_0 \partial T_c/\partial x = (\partial/\partial x)\kappa_c(\partial T_c/\partial x)$$
$$+ (\partial/\partial z)\kappa_c(\partial T_c/\partial z) + H_c, \tag{A8}$$

where u_0 is the velocity of the continent along the x-axis, and κ_c is the thermal diffusivity of the continent.

C. Boundary conditions

We assume continuity for the temperature and heat flow, and a non-slip boundary for the velocity $V_x = u_0$ and $V_z = 0$ at the bottom and

on the sides of the continent, respectively. As a result, eq. (6) may be simplified (Trubitsyn *et al.* 1999; Trubitsyn 2000b) to balance the pressure on the sides of the continent and viscous stresses on its bottom:

$$\int_{1-d}^{1} \left[(p)_{x=x_1+l} - (p)_{x=x_1} \right] dz + \int_{x_1}^{x_1+l} \eta (\partial V_x / \partial z)_{z=1-d} \, dx = 0.$$

$$(A9)$$

Thus, the unknowns to be found throughout the mantle are the velocity components $V_x(x, z)$ and $V_z(x, z)$, pressure $p(x, z)$, and temperature $T(x, z)$. Other unknowns sought for are the velocity $u_0(x)$, the temperature inside the continent $T_c(x, z)$ and the coordinate of its left side $x_1(t)$. These seven unknowns are found from the four convection equations, eqs (1)–(4), coupled with three equations for a moving plate, eqs (7)–(9). As these equations contain the large square terms $V_x \partial T / \partial x, V_z \partial T / \partial z$ and $u_0 \partial T_c / \partial x$, they are essentially non-linear.

In the case of a thin plate, the boundary condition (9) reduces to a simple balance of the viscous stresses at the continental bottom (Gable *et al.* 1991)

$$\int_{x_1}^{x_1+l} \eta (\partial V_x / \partial z)_{z=1-d} \, dx = 0. \qquad (A10)$$

D. Numerical scheme

The equations for the mantle convection and for the continent's motion are solved separately for each time step. The solutions are then finally adjusted to meet the boundary conditions at the mantle–continent interface. The numerical scheme may be summarized as follows.

At the initial time epoch t_0, the convective velocities $V(t_0)$, temperature $T(t_0)$, and pressure $p(t_0)$ in the mantle, as well as the position of the continent $x_c(t_0)$ and its velocity $u_0(t_0)$ are considered as known. Eqs (1)–(4) and (7)–(9) are then used to project these variables to the next time epoch $t_1 = t_0 + \Delta t$. The new position of the continent $x_c(t_1)$ is simply equal to $x_c(t_0) + u_0(t_0)\Delta t$. As soon as the new velocity of the continent $u_0(t_1)$ is known, the thermal convection equations, eqs (1)–(5) can be solved with the boundary conditions for the temperature and velocities corresponding to the new position of the continent. This gives the mantle flow velocities $V_x(t_1)$ and $V_y(t_1)$, the temperature $T(t_1)$, and the pressure $p(t_1)$. Thus the solution of one of the systems needs the solution of the other. The new mantle velocities $V_x(t_1)$ and $V_y(t_1)$ should be consistent with the equation of continental motion, eq. (9). To find unknown $u_0(t_1)$ we use trial and error method, whereby the convective velocities fit to the integral eq. (9) with a difference from zero less than $|\varepsilon|$. Here ε is a predefined number, that specifies the accuracy of the calculations. If the computed velocity of the continent $u_0(t_1)$ is underestimated, then $\varepsilon > 0$, otherwise $\varepsilon < 0$.

A finite difference method is used to solve the above given systems of equations (Trubitsyn & Rykov 1995). The flux-corrected transport algorithm of Zalesak (1979) is applied to solve the heat conservation equation, eq. (3). The equations for the velocities and pressure, eqs (1), (2) and (9), respectively, are reduced to elliptical equations with variable coefficients (generalized Poisson equations). They are solved using the three-layer modification of the triangular method and the method of conjugate gradients for chosen iteration parameters.